

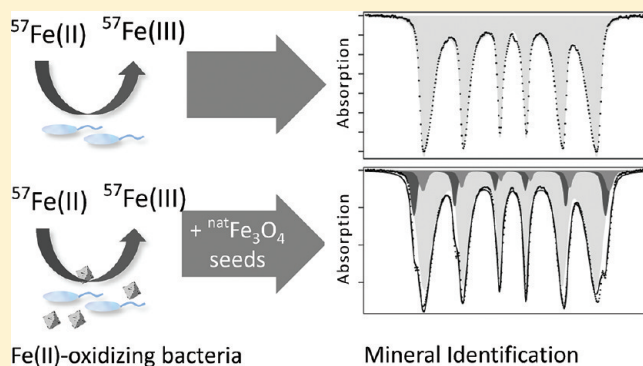
# Potential Function of Added Minerals as Nucleation Sites and Effect of Humic Substances on Mineral Formation by the Nitrate-Reducing Fe(II)-Oxidizer *Acidovorax* sp. BoFeN1

Urs Dippon, Claudia Pantke, Katharina Porsch,<sup>†</sup> Phil Larese-Casanova,<sup>‡</sup> and Andreas Kappler\*

Geomicrobiology, Center for Applied Geosciences, University of Tübingen, Sigwartstrasse 10, D-72076 Tübingen, Germany

## Supporting Information

**ABSTRACT:** The mobility of toxic metals and the transformation of organic pollutants in the environment are influenced and in many cases even controlled by iron minerals. Therefore knowing the factors influencing iron mineral formation and transformation by Fe(II)-oxidizing and Fe(III)-reducing bacteria is crucial for understanding the fate of contaminants and for the development of remediation technologies. In this study we followed mineral formation by the nitrate-reducing Fe(II)-oxidizing strain *Acidovorax* sp. BoFeN1 in the presence of the crystalline Fe(III) (oxyhydr)oxides goethite, magnetite and hematite added as potential nucleation sites. Mössbauer spectroscopy analysis of minerals precipitated by BoFeN1 in <sup>57</sup>Fe(II)-spiked microbial growth medium showed that goethite was formed in the absence of mineral additions as well as in the presence of goethite or hematite. The presence of magnetite minerals during Fe(II) oxidation induced the formation of magnetite in addition to goethite, while the addition of humic substances along with magnetite also led to goethite but no magnetite. This study showed that mineral formation not only depends on the aqueous geochemical conditions but can also be affected by the presence of mineral nucleation sites that initiate precipitation of the same underlying mineral phases.



## INTRODUCTION

Iron is one of the most ubiquitous elements in the earth's crust, and its biogeochemical cycling influences organic contaminant degradation as well as metalloid and heavy metal (im)-mobilization in sediments and soils.<sup>1</sup> Due to the low solubility of ferric iron (Fe(III)) at neutral pH, minerals form when dissolved ferrous iron (Fe(II)), which has a much higher solubility than Fe(III) and therefore can exist at significant concentrations at neutral pH, is oxidized to Fe(III). During this process, heavy metals and metalloids such as U or As can be coprecipitated with the iron minerals and thus are effectively immobilized.<sup>1,2</sup> However, the stability of microbially formed Fe(III) minerals against microbial and chemical reduction and dissolution varies considerably for different Fe(III) (oxyhydr)oxides such as ferrihydrite ( $\text{Fe}_{8.2}\text{O}_{8.5}(\text{OH})_{7.4}\cdot 3\text{H}_2\text{O}$ , simplified as  $\text{Fe}(\text{OH})_3$ ), goethite (alpha- $\text{FeOOH}$ ), magnetite ( $\text{Fe}_3\text{O}_4$ ) and hematite (alpha- $\text{Fe}_2\text{O}_3$ ). Reductive dissolution of these minerals can lead to remobilization of the sequestered contaminants. Due to the different solubilities and reactivities of the different Fe(III) minerals, an understanding of the parameters controlling the identity of the minerals formed during Fe(II) oxidation is important in assessing contaminant behavior and development of remediation strategies. For example, arsenic can be effectively removed from solution by coprecipitation during microbially mediated Fe(II) oxidation.<sup>3</sup> Depending on the stability of these solid phase As-bearing

Fe(III) (oxyhydr)oxides reduction by dissimilatory Fe(III)-reducing bacteria (DIRB) may again release As into the groundwater.<sup>4,5</sup>

In anoxic pH-neutral soils and sediments, iron redox processes are driven to a large extent by microbial activity.<sup>6–8</sup> DIRB can reduce a wide range of iron minerals including poorly crystalline oxides which are frequently found in soils.<sup>5</sup> Reoxidation of Fe(II) can occur chemically by oxygen or enzymatically catalyzed by different Fe(II)-oxidizing bacteria using oxygen or nitrate/nitrite as electron acceptor. Additionally, Fe(II) can be oxidized abiotically by nitrite, a byproduct of denitrifying bacteria. Depending on the habitat pH and redox conditions, either aerobic, microaerophilic or anaerobic (light-driven or nitrate-reducing) iron-oxidizing bacteria might prevail. In anoxic sediments, nitrate-reducing, Fe(II)-oxidizing bacteria can contribute to iron cycling and such bacteria have indeed been isolated from different habitats ranging from fresh water lake sediments to arsenic-rich aquifers.<sup>9–11</sup>

Biogenic iron minerals, formed either by DIRB or Fe(II)-oxidizing bacteria, are particularly important for contaminant remediation because (i) their small particle size provides a high

Received: December 22, 2011

Revised: May 17, 2012

Accepted: May 29, 2012

Published: May 29, 2012

**Table 1. Mössbauer Spectroscopy Results (Obtained at 140K) for Iron Minerals Formed During Fe(II) Oxidation by *Acidovorax* sp. BoFeN1 in the Presence of Different Iron Mineral Nucleation Sites and Humic Substances<sup>a</sup>**

sample	mineral seeds added [ $\mu\text{g/mL}$ ]	model <sup>b</sup>	center shift [mm/s]	quadrupole splitting [mm/s]	hyperfine field [T]	area [%]
no seeds	0	Fe(III) <sup>c</sup>	0.44	0.68		0.7
		goethite	0.47	-0.24	40.9	99.3
goethite	39	goethite	0.47	-0.24	41.1	100.0
hematite	156	siderite	1.32	2.24		13.5
		hematite <sup>d</sup>	0.46	0.40	53.5	1.3
magnetite	137	goethite	0.46	-0.24	42.2	85.2
		goethite	0.45	-0.22	43.4	84.5
		Mag Tet <sup>e</sup>	0.33	-0.04	50.4	9.3
		Mag Oct <sup>f</sup>	0.83	0.04	49.0	6.2
		sum magnetite (Tet and Oct) <sup>j</sup>				15.5
magnetite and humic substances [0.42 mg/mL]	137	Fe(III) <sup>g</sup>	0.45	0.65		12.6
		goethite <sup>h</sup>	0.45	-0.22	38.7	87.4
		magnetite	n.d.	n.d.	n.d.	n.d.
magnetite No BoFeN1; Fe(II) oxidation by H <sub>2</sub> O <sub>2</sub>	137	Fe(III) <sup>i</sup>	0.53	0.70		66.0
		Fe(II) <sup>i</sup>	1.20	2.50		30.0
		Mag Tet <sup>e</sup>	0.33	-0.08	50.7	2.3
		Mag Oct <sup>f</sup>	0.84	0.08	49.0	1.6
		sum magnetite (Tet and Oct) <sup>k</sup>				3.9

<sup>a</sup>The amounts of seeds added were normalized to the same number of surface sites in all setups. In the sterile control (no BoFeN1 cells) the Fe(II) was oxidized by H<sub>2</sub>O<sub>2</sub>. Area gives model results for the respective mineral phases in % of <sup>57</sup>Fe present in the respective sample. n.d.: not detectable (below detection limit). <sup>b</sup>Spectral data was modeled using Voigt-based spectral lines. The models for (super)paramagnetic phases comprise two peaks (doublet) for magnetically split phases showing a hyperfine field six peaks (sextet). Each spectral fit is a linear combination of the respective models. <sup>c</sup>Poorly crystalline Fe(III), most probably ferrihydrite. <sup>d</sup>Hematite originating from added nucleation sites. Calculations based on the initial <sup>57</sup>Fe distribution predict ~3% of the <sup>57</sup>Fe to be present in hematite. <sup>e</sup>Magnetite, tetrahedral sites, Fe oxidation state is Fe(III). <sup>f</sup>Magnetite, octahedral sites. Sites are populated by Fe(II) and Fe(III), with a ratio of 1:1 in stoichiometric magnetite. <sup>g</sup>Poorly crystalline Fe(III), most probably nanogoethite. <sup>h</sup>Poorly crystalline with significantly reduced hyperfine field compared to bulk goethite. <sup>i</sup>Poorly crystalline Fe(II) and Fe(III) which represent a mixture of carbonate green rusts, ferrihydrite and siderite. Due to the low crystallinity, an accurate distinction of single phases is not possible. 77K spectra of the same sample suggest ~48% carbonate green rust, ~33% ferrihydrite and ~14% siderite. <sup>j</sup>The initial magnetite nucleation sites contribute ~2–3% of spectral area (calculated on the basis of <sup>57</sup>Fe content) while the remaining 12.5–13.5% of the magnetite signal is attributed to minerals formed during Fe(II) oxidation. <sup>k</sup>Magnetite originating from added nucleation sites. Calculations based on the initial <sup>57</sup>Fe distribution predict 2–3% of the <sup>57</sup>Fe to be present in magnetite.

surface area for sorption and redox reactions<sup>12,13</sup> and (ii) their ability to coprecipitate contaminant metals. For example As immobilization was observed both during Fe(II) oxidation by nitrate-reducing Fe(II)-oxidizing bacteria<sup>3,14</sup> and during microbial Fe(III) reduction due to secondary Fe-mineral formation.<sup>15</sup>

The identity and the properties of biogenic minerals are strongly influenced by the geochemical conditions present during their formation. For Fe(III)-reducing bacteria, the influence of pH, the presence of dissolved ions such as phosphate, carbonate, or silicate, the presence of humic substances (HS) and extracellular polymeric substances, the cell to mineral ratio and the microbial reduction rate has been studied extensively.<sup>1,16–19</sup> Recently, interest in the parameters controlling mineral formation during microbial iron oxidation has increased. So far studies investigating iron mineral formation during microbial iron oxidation mainly focused on the influence of pH, dissolved organic compounds, ions or trace metals.<sup>20–25</sup> For *Acidovorax* sp. BoFeN1, it was shown that the identity of buffer used (bicarbonate or MOPS buffer) and the presence of phosphate influenced the mineralogy<sup>23</sup> and that the presence of As changed both the crystallinity and identity of the oxidation product.<sup>3</sup> The presence of dissolved organic compounds such as citrate, polysaccharides and HS was shown to influence the surface properties and particle size of the iron minerals formed during abiotic iron(III) hydrolysis and Fe(III) mineral precipitation<sup>26,27</sup> or even lead to a different mineralization product upon microbial Fe(II) oxidation.<sup>23</sup> In

natural environments such as soils and lake sediments, organic compounds such as HS are ubiquitously present and are therefore expected to influence the identity of microbial iron oxidation products. During microbial Fe(III) reduction, dissolved and solid-phase HS can shuttle electrons between bacterial cells and mineral surfaces.<sup>28–31</sup> HS can also inhibit the growth of certain minerals or modify mineral transformation products through surface sorption during microbial iron reduction.<sup>17</sup> HS electron shuttling has not been described during microbial Fe(II) oxidation so far, and the influence of HS on mineral formation during microbial Fe(II) oxidation under growth conditions has not yet been studied systematically.

Another important constituent of environmental systems that potentially influence the products of microbial iron oxidation are existing Fe minerals. Such minerals can sorb nutrients and contaminants, at the same time the mineral surfaces can also act as nucleation sites for further crystal growth and thus influence the thermodynamics and kinetics of mineral formation and thus the identity of the mineral product. The continued growth of existing crystals requires less energy compared to homogeneous nucleation, that is, the spontaneous nucleation of new particles out of a supersaturated solution.<sup>32</sup> This leads to preferential growth of existing nucleation sites instead of formation of new crystallites. Seeding is a widely used technique used for crystal growth in industrial applications such as the production of fine chemicals, pharmaceuticals, the semiconductor industry,<sup>33,34</sup>

but also in the production of technical iron oxides for acid mine drainage remediation.<sup>35</sup> Mineral adsorbents can control the identity and morphology of the Fe(III) product formed during abiotic Fe(II) oxidation with metallic and organic contaminants.<sup>36–38</sup> However, the influence of mineral nucleation sites on the mineralogy of microbial Fe(II) oxidation in environments such as soils or lake sediments is unknown.

Therefore, the goal and the innovative aspect of the present study was to identify and quantify the minerals produced by *Acidovorax* sp. BoFeN1 in presence of mineral additions of goethite, hematite and magnetite that can potentially function as nucleation sites and to compare these results to setups without initially present minerals. Additionally, we investigated the influence of HS on the minerals formed in the presence of magnetite.

## MATERIALS AND METHODS

**Source of Microorganism.** Strain BoFeN1 is a chemoorganotrophic, nitrate-reducing  $\beta$ -Proteobacterium closely related to *Acidovorax* sp. isolated from Lake Constance sediments. BoFeN1 grows mixotrophically oxidizing ferrous iron with acetate as organic cosubstrate.<sup>9,39</sup>

**Microbial Growth Media and Growth Conditions.** For routine cultivation of strain BoFeN1, 10 mM Na-nitrate and 5 mM Na-acetate were added to 22 mM bicarbonate-buffered mineral medium (pH 7.1, for composition see Supporting Information (SI) Table S1), prepared anoxically as described in detail by Hegler et al. and Hohmann et al.<sup>3,40</sup> For mineral precipitation experiments, 10 mM Fe(II) from a sterile 1 M FeCl<sub>2</sub> stock solution was added followed by precipitation of whitish, poorly crystalline Fe(II) carbonates and Fe(II) phosphates.<sup>41</sup> Precipitate-free medium was then prepared by sterile filtration (0.22  $\mu$ m, mixed cellulose esters, Millipore) in an anoxic glovebox (Braun, 100% N<sub>2</sub> atmosphere) according to Kappler and Newman<sup>41</sup> and contained a final Fe(II) concentration of 6–8 mM and a remaining concentration of 10–20  $\mu$ M phosphate. This precipitate-free medium is still oversaturated in respect to siderite (SI Table S2) but due to the slow kinetics of siderite precipitation<sup>42</sup> only little siderite precipitation was observed during microbial Fe(II) oxidation and all Fe(III) minerals present can be attributed to microbial activity.

**Nucleation Site Minerals and <sup>57</sup>Fe Solution.** In order to discriminate between the initially present mineral phases (seed minerals) and newly formed biogenic minerals, we used seed minerals of natural isotopic composition (2.2% <sup>57</sup>Fe) and <sup>57</sup>Fe(II) enriched growth media in combination with <sup>57</sup>Fe-Mössbauer spectroscopy in order to identify and quantify newly formed minerals by their enhanced signal strength. <sup>57</sup>Fe(II) solution (500 mM) was obtained by dissolving 95% pure <sup>57</sup>Fe(0) metal (Chemgas) in anoxic 1 M HCl within an anoxic glovebox (Braun, 100% N<sub>2</sub> atmosphere). The solution was filtered (0.45  $\mu$ m, mixed cellulose esters, Millipore) to remove possible particulate residues. As nucleation sites, commercially available goethite (specific surface area (ssa) = 9.2 m<sup>2</sup> g<sup>-1</sup>, 2 surface sites nm<sup>-2</sup>, 0.6–0.9  $\mu$ m length), hematite (ssa = 2.1 m<sup>2</sup> g<sup>-1</sup>, 3 surface sites nm<sup>-2</sup>, 0.1–0.3  $\mu$ m) and magnetite (ssa = 3.8 m<sup>2</sup> g<sup>-1</sup>, 2.2 surface sites nm<sup>-2</sup>, 0.3–0.6  $\mu$ m) were used (Lanxess). In order to provide the same amount of surface sites for nucleation, the amount of nucleation site minerals was adjusted according to the respective specific surface area and surface site densities of the minerals to provide 4  $\times$  10<sup>16</sup> surface

sites per mL of final medium. The amounts of mineral seeds added are given in Table 1. For the experiments, a 50 $\times$  stock suspension of each mineral (22 mM for goethite, 49 mM for hematite, and 30 mM for magnetite) was prepared in sterile demineralized water and deoxygenized by alternating application of vacuum and N<sub>2</sub>. Aliquots of the stock suspension were then transferred, while agitated to homogenize the suspension, to the experimental bottles in the glovebox.

**Humic Substance Solution.** Pahokee peat humic acids (PPHA) were purchased from the International Humic Substance Society. The PPHA were dissolved in 88.6 mM NaCl solution to a final concentration of 10 mg/mL and pH was adjusted to 7.0 using NaOH. The stock solution was sterile filtered (0.22  $\mu$ m, mixed cellulose esters, Millipore) and deoxygenized by alternating application of vacuum and N<sub>2</sub>.

**Experimental Setup.** Serum bottles (58 mL) were rinsed with 1 M HCl and distilled water prior to sterilization in order to obtain uniform surface properties of the glass. Twenty-five mL of filtered medium was filled anoxically into each bottle; the bottles were flushed with N<sub>2</sub>/CO<sub>2</sub> (90/10), closed with a butyl stopper and crimped. Each bottle was spiked with 75  $\mu$ L of anoxic <sup>57</sup>Fe(II) stock solution (500 mM) and 0.5 mL of 50 $\times$  nucleation site suspension. The inoculum was 1.25 mL of an iron-free BoFeN1 culture (grown with acetate/nitrate only) and the culture bottles were incubated for 12–14 days at 28  $^{\circ}$ C. All treatments were set up in replicate bottles. For mineral analysis representative bottles were chosen. Controls using sterile medium including nucleation sites were either chemically oxidized with 100  $\mu$ L of 35% H<sub>2</sub>O<sub>2</sub> (Acros Organics) and incubated for 7 days at 28  $^{\circ}$ C or incubated without oxidation at 28  $^{\circ}$ C for 12–14 days. H<sub>2</sub>O<sub>2</sub> as chemical oxidant was chosen to avoid secondary effects by other ions introduced such as, for example, Mn from permanganate and to provide fast and complete oxidation.

**Analytical Methods.** For quantification of total Fe(II) and Fe(III), 100  $\mu$ L of culture suspension were withdrawn anoxically with a syringe via a needle and added to 900  $\mu$ L of 1 M HCl for 24 h at room temperature. After dissolution of the biogenic minerals (the nucleation site material did not dissolve completely), iron was quantified by the ferrozine assay.<sup>43</sup>

For Mössbauer spectroscopic mineral analysis, biologically formed mineral precipitates were filtered (0.45  $\mu$ m, mixed cellulose esters, Millipore) in an anoxic glovebox (100% N<sub>2</sub>). Size exclusion during the filtration step was not expected since iron oxide particles down to a size of  $\sim$ 7 nm were effectively immobilized on the membranes (indicated by the clear filtrate in our experiments). The filters were sealed between two layers of oxygen-impermeable adhesive polyimide film (Kapton) in the glovebox. Samples were mounted in a close-cycle exchange-gas cryostat (Janis cryogenics) that allowed stepwise cooling of the sample to 4.5 K. The samples were analyzed at 140, 77, and 4.5 K. Mössbauer spectra were collected with a constant acceleration drive system in transmission mode and with a <sup>57</sup>Co source (WissEL). Spectra were calibrated against a spectrum of alpha-Fe metal foil collected at room temperature. Spectra calibration and fitting was performed with Recoil software (University of Ottawa) using Voigt based spectral lines.

Samples for SEM were taken anoxically from the bottles, filtered onto 0.22  $\mu$ m pore size polycarbonate filters (Whatman), washed twice with anoxic demineralized water and dried under anoxic conditions. Samples were sputter coated with 8–9 nm Pt (BAL-TEC SCD 005/CEA 035, Bal-Tec, now Leica), and images were taken using a LEO 1450vp microscope (LEO

electronics, Ltd., now Zeiss SMP) with an acceleration of 10 KeV.

## RESULTS

Microbial Fe(II) oxidation by the nitrate-reducing Fe(II)-oxidizer *Acidovorax* sp. BoFeN1 was studied in the presence of added goethite, hematite, and magnetite minerals in order to determine their ability function as nucleation sites and their influence on Fe(II) oxidation mineral products. *Acidovorax* sp. BoFeN1 oxidized ~6 mM Fe(II) within one week both in the absence and presence of added minerals (Figure 1), which is

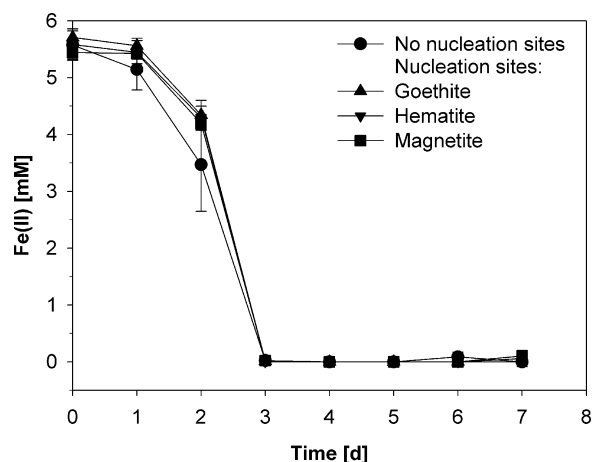


**Figure 1.** Oxidation of Fe(II) by the nitrate-reducing Fe(II)-oxidizing strain *Acidovorax* sp. BoFeN1 in the absence of nucleation sites and in the presence of goethite, hematite, and magnetite nucleation seeds, respectively. Oxidation was followed until the dissolved Fe(II) in the growth medium was fully oxidized. Mössbauer spectroscopy analysis of mineral products was performed 9–11 days after complete oxidation. Error bars indicate standard deviation of three parallel cultures.

consistent with previous rates of Fe(II) oxidation published for this strain.<sup>9,39</sup> This suggests that the presence of the minerals did not change Fe(II) availability for the microbial cells significantly (e.g., via surface complexation of Fe(II) by the mineral seeds) and did not have any negative or positive effect on Fe metabolism. From this data, we conclude that (i) the oxidation rate and thus the Fe(III) formation rate was the same in all experiments, and (ii) all differences observed in mineralogy are solely due to the presence of the mineral nucleation sites and are not related to different Fe(II) oxidation rates caused by the addition of the minerals.

Mössbauer spectra of minerals formed by BoFeN1 in the absence of any mineral addition showed goethite as the sole iron oxidation product (Figure 2A and Table 1 for Mössbauer modeling parameters). This is in agreement with previous findings for BoFeN1 in bicarbonate buffered growth media.<sup>3,23</sup> When adding goethite as nucleation sites, again goethite was the sole product of Fe(II) oxidation (Figure 2B). Addition of hematite to Fe(II)-containing medium inoculated with BoFeN1 did not initiate any hematite formation during Fe(II) oxidation. Hematite visible in the spectrum (1.3% of the spectral area in the mineral products) can be attributed to the <sup>57</sup>Fe naturally present in the initially added hematite material (Figure 2E). Instead of additional hematite, goethite was formed as Fe(III) phase in the presence of hematite plus some additional siderite (13.5%) that was probably precipitated due to Fe(II)-bicarbonate supersaturation from the medium.

In contrast, after Fe(II) oxidation by BoFeN1 in the presence of magnetite, Mössbauer spectra of the mineral products demonstrated that about 15.5% of the Fe in the precipitates was present in form of magnetite in addition to a large fraction of Fe present as goethite (Figure 2C). The amount of <sup>57</sup>Fe from the initially present magnetite that served as nucleation sites accounts for 2–3% of the spectral area (calculated from the distribution of <sup>57</sup>Fe and <sup>56</sup>Fe in all dissolved and precipitated Fe compounds in the system). The amount of 15.5% spectral area thus represents a five to six-fold increase in the <sup>57</sup>Fe magnetite signal. Sterile controls with <sup>57</sup>Fe(II) and <sup>56</sup>Fe(II) that were oxidized by H<sub>2</sub>O<sub>2</sub> within a few minutes and then incubated for 7 days show 4% magnetite under otherwise the same geochemical conditions as the biotic experiments (Figure 2F). The amount of <sup>57</sup>Fe from the initial magnetite in the sterile controls accounts for 2–3% (calculated from the distribution of <sup>57</sup>Fe and <sup>56</sup>Fe in all dissolved and precipitated Fe compounds in the system), which means that no significant magnetite formation took place in these abiotic Fe(II) oxidation experiments while the slower oxidation of Fe(II) to Fe(III) by BoFeN1 in the presence of initially added magnetite lead to crystallization of magnetite (Figure 2C). The poorly crystalline precipitates from the chemically oxidized control (H<sub>2</sub>O<sub>2</sub>) consisted of 66% Fe(III) and 30% Fe(II) and form a mixture of carbonate green rusts, ferrihydrite, and siderite but not goethite (Figure 2F). The individual minerals in this mixture could not be quantified separately due to overlapping features in the Mössbauer spectra.

Because only magnetite and not hematite or goethite resulted in the formation of a new mineral (magnetite) in addition to goethite, the effect of humic substances was investigated only for the magnetite nucleation site experiments. When adding humic substances to magnetite-seeded setups containing BoFeN1 cells, the Fe(II) oxidation rates did not change based on Fe(II) quantification after 5 days (data not shown), and no magnetite but rather poorly crystalline goethite (87.4%) and a paramagnetic phase similar to nanosized goethite (12.6%) was formed (Figure 2D).

Abiotic sterile controls with either goethite, hematite or magnetite seeds that were incubated in Fe(II)-containing growth medium for two weeks but not chemically oxidized by H<sub>2</sub>O<sub>2</sub> showed formation of small amounts of siderite (Figure 3). Siderite precipitation is expected in aged growth medium that is oversaturated with bicarbonate and Fe(II)<sub>dissolved</sub> (SI Table S2). A second Fe(II) doublet was present in the spectra of the abiotic sterile controls that did not resemble vivianite [Fe<sub>3</sub>(PO<sub>4</sub>)<sub>2</sub>·8H<sub>2</sub>O]. This doublet was in fact observed in all spectra that contained siderite precipitated within Fe(II)-rich media, that is, also in the microbially active hematite setup. This doublet has not been definitively identified but is labeled “siderite-associated Fe(II)” in Figures 2 and 3. One potential candidate is chukanovite (ferrous hydroxy carbonate).<sup>16,44</sup> In addition to the Fe(II) solids, the initially added minerals were clearly visible in the respective Mössbauer spectra of the sterile controls (Figure 3). This suggests that the added minerals were stable in the medium over the course of the experiments.

Electron microscopy analysis of magnetite used as nucleation site material before (Figure 4A) and after incubation for 14 days in sterile, nonoxidized controls showed precipitation of small amounts of minerals after 14 days. This was most probably siderite (and potentially other carbonates), stemming from the medium being oversaturated with bicarbonate and ferrous iron (Figure 4B, arrow labeled 1; SI Table S2). Siderite

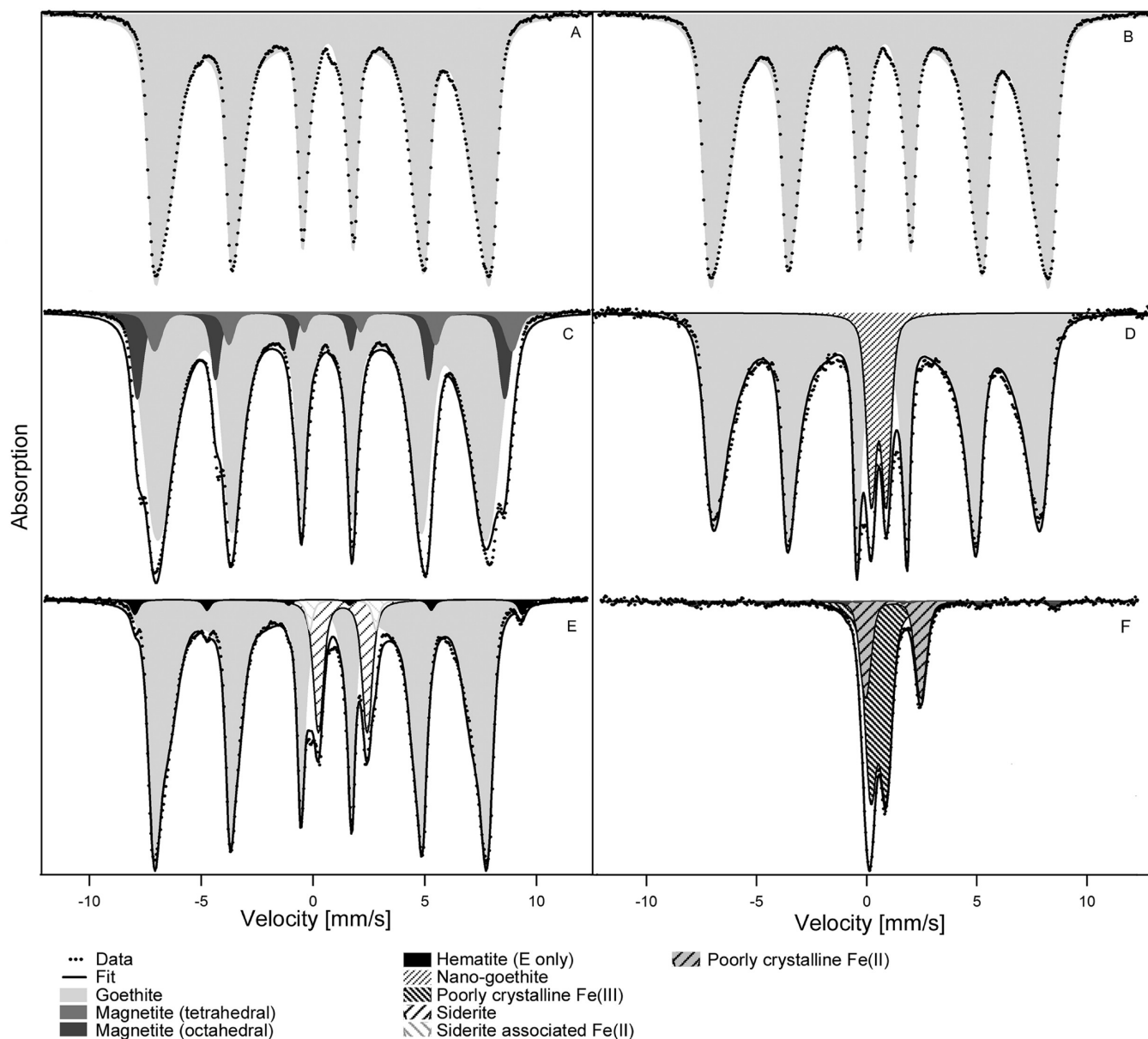


**Figure 2.**  $^{57}\text{Fe}$  Mössbauer spectra (measured at 140K) of minerals resulting after oxidation of approximately 6 mM of  $^{57}\text{Fe}$ -enriched Fe(II) by *Acidovorax* sp. BoFeN1. Minerals were collected from representative bottles 9–11 days after full oxidation of the dissolved Fe(II) present in the growth medium. (A) without additions, (B) in the presence of goethite, (C) in the presence of magnetite, (D) in the presence of magnetite plus 0.42 mg mL<sup>-1</sup> humic substances, and (E) in the presence of hematite. (F) Sterile control in the presence of magnetite with dissolved Fe(II) being partially oxidized using H<sub>2</sub>O<sub>2</sub>.

precipitation was confirmed as described above by Mössbauer spectroscopy (Figure 3C). The electron micrographs also showed that the magnetite crystals incubated in growth medium under sterile conditions did not change in morphology (Figure 4A and B). Micrographs from biotic setups containing BoFeN1, magnetite and Fe(II) taken after complete oxidation of the Fe(II) showed the formation of cell-mineral aggregates that were dominated by needle-like minerals that were closely associated with cells or even encrusting the cells (Figure 4C). Distinct octahedral magnetite crystals were only found in some images. The lower abundance of magnetite in comparison to encrusted cells within the images matches the observations within Mössbauer spectra, which showed that the  $^{57}\text{Fe}$ (II) precipitated to 84.5% as goethite, which has a needle-like

morphology, and 15.5% was present as magnetite upon oxidation.

## DISCUSSION

The geochemical and microbiological influences on iron mineral transformation in soil and sediments have been subject to extensive investigations due to the importance of iron minerals in nutrient cycling and contaminant remediation.<sup>1,6–8,45</sup> Due to the complex composition of soils and sediments (e.g., mineral particles of various composition and size, biota, humic substances, fluctuating geochemical conditions, etc.), most of these studies used simplified laboratory systems, and many questions related to heterogeneous systems remain unresolved, for example, the combined effect of dissolved HS and added minerals. The aim of the present

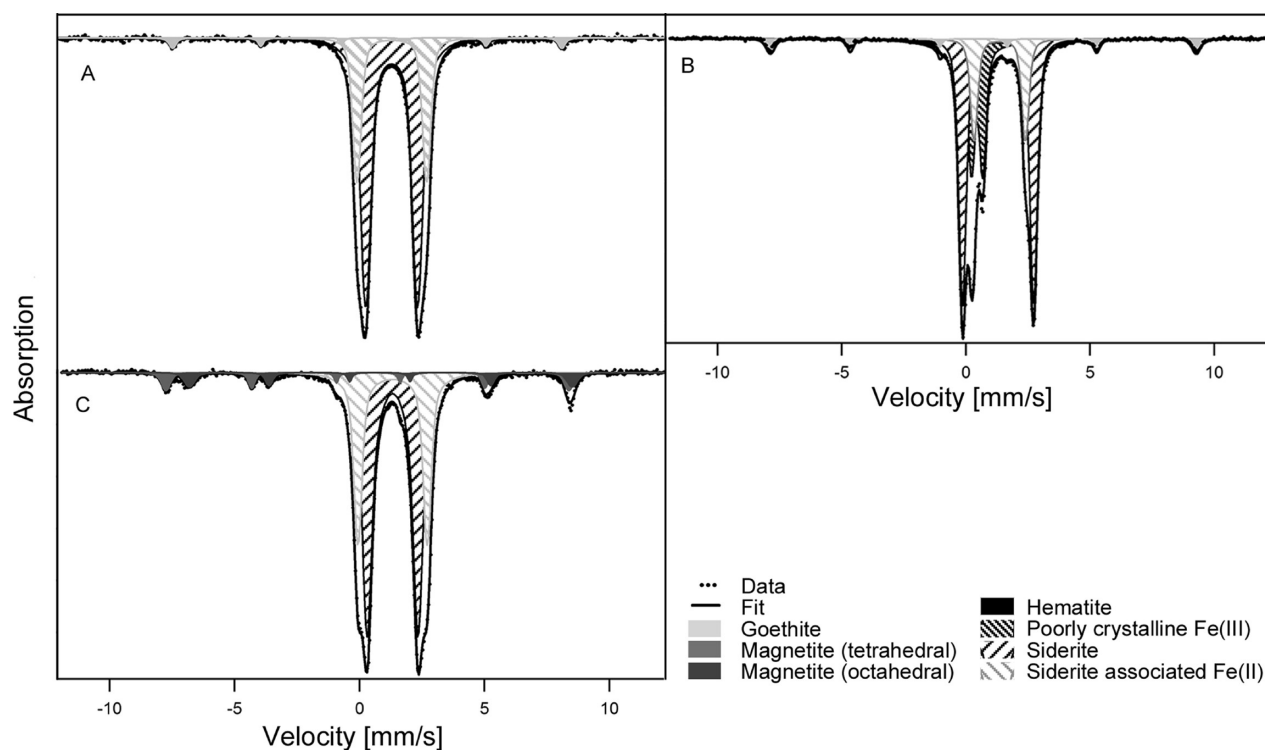


**Figure 3.**  $^{57}\text{Fe}$  Mössbauer spectra (measured at 140K) of minerals resulting after aging of  $\sim 6$  mM of  $^{57}\text{Fe}$ -enriched Fe(II) medium for 14 days in the presence of mineral nucleation sites goethite (A), hematite (B), and magnetite (C).

study was to investigate whether the presence of different iron (oxyhydr)oxide mineral phases during Fe(II) oxidation by the nitrate-reducing Fe(II)-oxidizing strain *Acidovorax* sp. BoFeN1 influences the identity of the iron minerals formed during Fe(II) oxidation.

**Mineral Formation by *Acidovorax* sp. BoFeN1 under Different Geochemical Conditions.** In the absence of minerals, during oxidation of dissolved Fe(II) in bicarbonate buffered mineral media that contained low concentrations of phosphate ( $<1$  mM), strain BoFeN1 and a related *Acidovorax* strain sp. 2AN were previously shown to encrust its cells with a layer of small, needle-like goethite particles.<sup>3,9,46</sup> The present study confirmed these findings and identified goethite as the mineral product after complete Fe(II) oxidation in comparable growth medium (Figures 2A and 4C). Goethite formation in bicarbonate-buffered mineral medium was also observed as one of the end products of Fe(II) oxidation by other anaerobic Fe(II)-oxidizing bacteria.<sup>41,47,48</sup> However, goethite is not the only mineral that is precipitated by strain BoFeN1. Carbonate green rust was detected in BoFeN1 cultures as intermediate phase during the first two days of Fe(II) oxidation.<sup>49</sup> In the presence of several mM of dissolved phosphate or in the initial presence of the Fe(II)-phosphate vivianite, the Fe(II) oxidation product consisted mainly of amorphous Fe(III)-phosphates.<sup>24,50</sup>

Additionally, metal ions such as As(III) and As(V) were shown to influence the identity and crystallinity of the mineralization product. In particular increasing As(V) concentrations led to a decrease in crystallinity of the minerals and to the formation of a mineral mixture consisting of goethite and ferrihydrite.<sup>3</sup> In another study, cell suspension experiments with BoFeN1 without growth medium showed that the mineralogy of Fe(II) oxidation is also influenced by the buffer system used, as lepidocrocite formed instead of goethite when bicarbonate

was replaced by organic MOPS buffer,<sup>23</sup> which is consistent with results from abiotic mineral synthesis experiments where the presence of  $\text{CO}_2$  was shown to promote goethite formation at the expense of lepidocrocite formation.<sup>51,52</sup> In summary, the above studies demonstrate that the mineral formation during Fe(II) oxidation in BoFeN1 cultures strongly depends on the solution chemistry. On the other hand, the occurrence of the metastable intermediate green rust before the formation of the final oxidation product goethite suggests that slow kinetics of mineral formation during Fe(II) oxidation control mineral identity as well.<sup>49</sup>

**Consequences of Kinetic Constraints on Microbial Fe(II) Oxidation Products.** While the geochemical conditions during Fe(II) oxidation are expected to ultimately control the mineral (trans)formation pathways leading to the thermodynamically most stable mineralization product under the given conditions, kinetic factors have to be considered as well. The thermodynamically most favorable product may not form due to a higher activation energy required compared to a less stable product.<sup>53</sup> Particularly when Fe(III) production rates are much too fast to allow equilibrium between the reactant (i.e.,  $\text{Fe}^{2+}$ ), the initial oxidation product (i.e.,  $\text{Fe}^{3+}$  formed during the oxidation process) and the final reaction products (i.e., Fe(III) minerals), the formation of poorly ordered phases is favored over the thermodynamically stable, highly crystalline product.<sup>53</sup> In the presented experiments rapid abiotic oxidation of 7 mM Fe(II) by  $\text{H}_2\text{O}_2$  within a few minutes in the presence of magnetite led to the formation of only poorly crystalline mineral phases (Figure 2F), which were impossible to be identified and quantified individually. In contrast, much slower microbial oxidation by BoFeN1 with maximum rates of  $<4$  mM per day (Figure 1) led, probably via some intermediate green rust formation,<sup>49</sup> both in the presence and absence of added

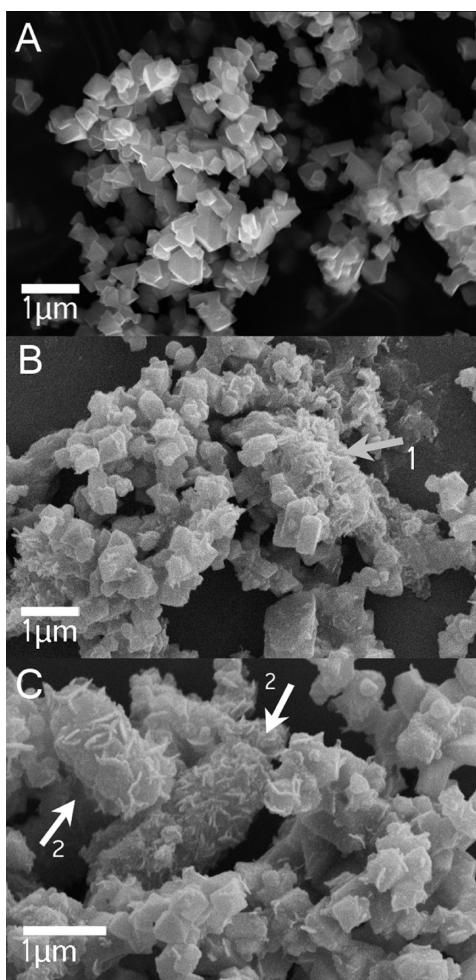


**Figure 4.** SEM micrographs of (A) magnetite nucleation site minerals before incubation, and (B) magnetite nucleation sites in sterile controls aged for 14 days in 22 mM bicarbonate buffered growth medium. Arrow labeled “1” points to precipitates, most probably siderite, which formed due to the oversaturation of the medium with bicarbonate (see also Figure 3). (C) Minerals formed in *Acidovorax* sp. BoFeN1 cultures seeded with magnetite after 5 days of incubation. Arrows labeled “2” point to mineral encrusted *Acidovorax* sp. BoFeN1 cells.

minerals to crystalline goethite and goethite-magnetite mixtures, respectively (Figure 2A–E).

It has to be noted that magnetite is stable under the experimental conditions (Figures 3C and 4), and because it was suggested that BoFeN1 can only utilize dissolved Fe(II),<sup>50</sup> we do not expect magnetite to be oxidized by BoFeN1. This means that both goethite and magnetite form in parallel either directly from dissolved Fe(II) and Fe(III) or from less stable precursors like ferrihydrite or green rusts. Magnetite formation is thermodynamically favorable in many experimental systems containing both Fe(II) and Fe(III), and during microbial Fe(III) reduction magnetite formation is indeed commonly observed.<sup>54</sup> The transformation process is thought to be topotactic solid state conversion of ferrihydrite induced by sorbed Fe(II).<sup>51,54,55</sup> In contrast, during microbial Fe(II) oxidation, magnetite formation has only been described for the phototrophic Fe(II)-oxidizer *Rhodospseudomonas palustris* strain TIE1<sup>56</sup> and the Fe(II)-oxidizing strain *Azospira oryzae* PS,<sup>57</sup> although in the latter case the evidence for magnetite from the provided XRD diffractograms is questionable. The

reason why magnetite formation is kinetically hindered (although thermodynamically expected) during microbial Fe(II) oxidation could be that (i) different rates of Fe(II) oxidation lead to different local Fe(II)/Fe(III) ratios compared to microbial Fe(III) reduction or (ii) the initial lack of large amounts of solid Fe(III) phases prevents topotactic solid state conversion to magnetite as observed during ferrihydrite reduction. Evidence that kinetic factors influence biogenic iron mineral transformation is also found for microbial Fe(III) reduction. Under flow through conditions, low ferrihydrite reduction rates lead to goethite formation while faster rates lead to magnetite formation.<sup>58</sup> Based on similar results, Zachara<sup>19</sup> suggested a conceptual model where reduction rates control the mineralogy during microbial hydrous ferric oxide reduction with high ferrihydrite reduction rates leading to the formation of siderite, intermediate rates leading to magnetite and low rates to the more stable Fe(III) oxyhydroxides goethite via a dissolution reprecipitation mechanism. These observations illustrate how a combination of kinetics and thermodynamics controls the mineralization process during microbial iron redox transformation.

**Influence of Mineral Addition on the Kinetics of Mineral Precipitation and Transformation.** In systems where kinetic constraints influence mineral formation, nucleation sites can have a significant influence on mineralization since they eliminate the activation energy necessary for spontaneous nucleation of certain minerals, which is higher compared to energy necessary for growth of existing particles.<sup>33</sup> However, providing seeding crystals does not guarantee homoepitactic growth, that is, the mineral growing on the nucleation site may be different from the seed. For this process, termed heteroepitactic growth, the crystallographic lattice parameters of the seeding phase and the epitactic growing phase need to match in distance, with a few percent deviation being possible.<sup>33</sup>

Besides mineral surfaces, organic matrices (including microbially produced EPS or microbially produced cellular appendices, i.e., organic fibres) can also act as templates for mineral nucleation.<sup>22,59</sup> Additionally, negatively charged microbial cell surfaces attract metal cations and positively charged colloidal mineral precipitates, initiating mineral precipitation at the cell surface. Such a scenario is envisioned for strain BoFeN1 where cell encrustation in Fe(III) minerals is observed after Fe(II) oxidation in initially particle free, filtered medium. The minerals added in our experiments therefore compete with the cell surfaces for mineral nucleation.

In our experiments, Mössbauer spectroscopy did not show changes in mineral identity or crystallinity due to the addition of goethite as potential nucleation sites (Figure 2A and B). BoFeN1 cells became encrusted also in the presence of goethite seeds, which suggest the cell surface of BoFeN1 provides favorable conditions for mineral nucleation and growth in spite of a competitive goethite surface. However, it was not possible to quantify the amount of goethite encrusting the cells vs the total amount of goethite formed. For magnetite nucleation sites we could show that these did initiate magnetite formation during Fe(II) oxidation by BoFeN1, while the addition of hematite did not initiate formation of hematite but rather lead to goethite formation. This is somewhat unexpected since hematite formation during oxidation of Fe(II) (with the underlying hematite functioning as the oxidant) was described previously.<sup>60,61</sup> The reason for this difference is currently unclear.

SEM images of cultures containing magnetite seeds showed that precipitates on the cells after complete Fe(II) oxidation (Figure 3C) look morphologically similar to the goethite encrustations formed without nucleation sites.<sup>3,9,39</sup> Combined SEM and Mössbauer spectroscopy results suggest they are most likely goethite. Thus the mineral precipitation at the cell surface is not altered by the magnetite nucleation sites. The increase in magnetite content in the magnetite seeded Fe(II) oxidation cultures is therefore likely to be due to growth of the magnetite seeds. However, Mössbauer spectroscopy as a bulk technique does not allow spatially resolved analysis of mineral identity. Future studies employing synchrotron based STXM would potentially allow for mineral identification at the oxide surface.

The hypothesis that the magnetite nucleation sites grow and no magnetite precipitation occurs at the cell surface or in the periplasm has important implications for the Fe(II) oxidation mechanism. For strain BoFeN1 it was suggested that Fe(II) is oxidized in the periplasm.<sup>24</sup> In a recent report, Miot et al.<sup>62</sup> showed that the encrustation of BoFeN1 cells begins to form at the plasma membrane and then grows into the periplasm. If Fe(II) is oxidized at the plasma membrane and at the same time the magnetite nucleation seeds grow (at a distance to the cells) this implies that Fe(III) is transported from the microbial cells to the mineral seeds, either in the form of complexed (dissolved) Fe(III) or as small colloids. Indeed, flow-chamber experiments using the nitrate-reducing, Fe(II) oxidizing strain *Acidovorax* sp. 2AN did not show cell encrustation at Fe(II) concentrations below 250  $\mu\text{M}$  in contrast to batch experiments with mM concentrations of Fe(II), suggesting that a certain amount of Fe(III) can be transported away from the cell.<sup>46</sup> Assuming similar oxidation mechanisms for strain BoFeN1 and 2AN, it is therefore possible that some Fe(III) is transported from the periplasm out of the cell allowing the formation of magnetite at the magnetite seeds. Alternatively, nitrite, occurring as a metabolic intermediate during nitrate reduction with electrons stemming from acetate oxidation by the mixotrophic strain BoFeN1<sup>9</sup> could chemically oxidize Fe(II) at a distance from the cells, leading either to the growth of the magnetite nucleation sites or to metastable, mixed-valent mineral phases like green rust. Potential abiotic reactions occurring during microbial nitrate-dependent Fe(II) oxidation were discussed in detail in a recent paper by Picardal.<sup>63</sup> As a third possibility, the growth of the magnetite could be also promoted by recrystallization of metastable mineral phases such as green rusts.<sup>9</sup> As mentioned above, carbonate green rust was recently identified as an intermediate mineral phase during Fe(II) oxidation by BoFeN1.<sup>49</sup> Transformation of carbonate green rust phases to a variety of more stable mixed valent or ferric iron (hydr)oxides was described, among others to magnetite, goethite and hematite.<sup>51,57,64</sup> Thus, carbonate green rusts, which may form during the first days of Fe(II) oxidation by BoFeN1 can be considered as a source for both goethite formation and growth of magnetite crystals.

**Influence of Humic Substances.** Humic substances (HS) are typically negatively charged in pH-neutral medium and can therefore sorb to the surfaces of iron minerals that are positively charged under neutral conditions such as ferrihydrite (pzc 7.8–7.9), goethite (pzc 7.5–9.5), and magnetite (pzc 6.3–7.1).<sup>51,65,66</sup> As a consequence of these interactions, the mineral surface properties are altered and therefore influences on further mineral transformations are expected. In the particular case where HS were added to growth medium that contained magnetite nucleation sites, HS first inhibited magnetite

formation probably by binding of Fe(III) formed during Fe(II) oxidation and particularly by preventing Fe(II) sorption to the initially formed Fe(III) phase thus preventing the topotactic conversion of these Fe(III) phases to magnetite. Second, HS present during mineral precipitation become coprecipitated with the iron minerals, thereby disrupting the crystalline order or restricting increase of the particle size, as it was shown for HS as well as for other organic compounds.<sup>23,26,27,67,68</sup> Larese-Casanova<sup>23</sup> showed for MOPS-buffered (carbonate-free) BoFeN1 cell suspensions a significant influence of HS at concentrations above 1 mM DOC in nucleation site-free experiments where goethite replaced lepidocrocite as dominant phase and the overall mineral crystallinity decreased. The HS concentration of 0.42 mg HS mL<sup>-1</sup> in our experiments corresponds to a DOC concentration of ~17.5 mM, which is nearly 6-fold higher than the highest DOC concentration used by Larese-Casanova.<sup>23</sup> And indeed, Mössbauer spectroscopy analysis of the goethite formed in the presence of HS showed a significant decrease of the average magnetic hyperfine field for the goethite itself and additionally suggested the formation of nanogoethite (Table 1), both evidence for a lower crystallinity of the mineral products.

## ■ CONCLUSIONS

In this study we showed that the presence of existing mineral surfaces during biomineralization can change the biomineralization products, as magnetite seeds triggered further magnetite formation during oxidation of Fe(II) by bacteria that otherwise did not produce magnetite. Humic substances inhibited this process probably by a surface coating. Furthermore, it was shown that not all mineral seeds tested triggered homoepitaxial growth, so the ability to serve as nucleation site depends on mineral specific properties. The demonstrated influence of nucleation sites on mineral products formed by the Fe(II)-oxidizing nitrate-reducing strain BoFeN1 is helpful in interpreting the larger phenomena of microbial Fe(II) oxidation, biomineral formation, geochemical controls, and the consequences of microbial mineral formation for nutrients and pollutants in the environment.

## ■ ASSOCIATED CONTENT

### 📄 Supporting Information

Supporting Information including Tables S1 and S2. This material is available free of charge via the Internet at <http://pubs.acs.org>.

## ■ AUTHOR INFORMATION

### Corresponding Author

\*Phone: +49-7071-2974992; fax: +49-7071-29-295059; e-mail: andreas.kappler@uni-tuebingen.de.

### Present Addresses

† Department of Bioenergy, Helmholtz Centre for Environmental Research – UFZ, Leipzig, Germany

‡ Department of Civil and Environmental Engineering, Northeastern University, Boston, Massachusetts, United States

### Notes

The authors declare no competing financial interest.

## ■ ACKNOWLEDGMENTS

This work was supported by research proposals (KA 1736/14-1 and 16-1) from the German Research Foundation (DFG) to A.K. and by BMBF “IPSWaT” PhD fellowships to C.P. and



U.D. We thank N. Hagemann for help with SEM imaging, A. Buchholz for BET measurements, and F. Hegler for phosphate quantification. The authors also thank three anonymous reviewers for helpful comments.

## REFERENCES

- (1) Borch, T.; Kretzschmar, R.; Kappler, A.; Van Cappellen, P.; Ginder-Vogel, M.; Voegelin, A.; Campbell, K. Biogeochemical redox processes and their impact on contaminant dynamics. *Environ. Sci. Technol.* **2010**, *44* (1), 15–23.
- (2) Lack, J. G.; Chaudhuri, S. K.; Kelly, S. D.; Kemner, K. M.; O'Connor, S. M.; Coates, J. D. Immobilization of radionuclides and heavy metals through anaerobic bio-oxidation of Fe(II). *Appl. Environ. Microbiol.* **2002**, *68* (6), 2704–2710.
- (3) Hohmann, C.; Winkler, E.; Morin, G.; Kappler, A. Anaerobic Fe(II)-oxidizing bacteria show As resistance and immobilize As during Fe(III) mineral precipitation. *Environ. Sci. Technol.* **2010**, *44* (1), 94–101.
- (4) Cummings, D. E.; Caccavo, F.; Fendorf, S.; Rosenzweig, R. F. Arsenic mobilization by the dissimilatory Fe(III)-reducing bacterium *Shewanella alga* BrY. *Environ. Sci. Technol.* **1999**, *33* (5), 723–729.
- (5) Roden, E. E.; Zachara, J. M. Microbial reduction of crystalline iron(III) oxides: Influence of oxide surface area and potential for cell growth. *Environ. Sci. Technol.* **1996**, *30* (5), 1618–1628.
- (6) Fortin, D.; Langley, S. Formation and occurrence of biogenic iron-rich minerals. *Earth. Sci. Rev.* **2005**, *72* (1–2), 1–19.
- (7) Kappler, A.; Straub, K. L. Geomicrobiological cycling of iron. *Rev. Mineral. Geochem.* **2005**, *59*, 85–108.
- (8) Konhauser, K. O.; Kappler, A.; Roden, E. E. Iron in microbial metabolisms. *Elements* **2011**, *7* (2), 89–93.
- (9) Kappler, A.; Schink, B.; Newman, D. K. Fe(III) mineral formation and cell encrustation by the nitrate-dependent Fe(II)-oxidizer strain BoFeN1. *Geobiology* **2005**, *3*, 235–245.
- (10) Sutton, N. B.; van der Kraan, G. M.; van Loosdrecht, M. C. M.; Muyzer, G.; Bruining, J.; Schotting, R. J. Characterization of geochemical constituents and bacterial populations associated with As mobilization in deep and shallow tube wells in Bangladesh. *Water Res.* **2009**, *43* (6), 1720–1730.
- (11) Weber, K. A.; Pollock, J.; Cole, K. A.; O'Connor, S. M.; Achenbach, L. A.; Coates, J. D. Anaerobic nitrate-dependent iron(II) bio-oxidation by a novel lithoautotrophic betaproteobacterium, strain 2002. *Appl. Environ. Microbiol.* **2006**, *72* (1), 686–694.
- (12) Martinez, C.; McBride, M. Coprecipitates of Cd, Cu, Pb, and Zn in iron oxides: Solid phase transformation and metal solubility after aging and thermal treatment. *Clay. Clay Miner.* **1998**, *46* (5), 537–545.
- (13) Neubauer, S. C.; Emerson, D.; Megonigal, J. P. Life at the energetic edge: Kinetics of circumneutral iron oxidation by lithotrophic iron-oxidizing bacteria isolated from the wetland-plant rhizosphere. *Appl. Environ. Microbiol.* **2002**, *68* (8), 3988–3995.
- (14) Hohmann, C.; Morin, G.; Ona-Nguema, G.; Guigner, J.-M.; Brown, G. E.; Kappler, A. Molecular-level modes of As binding to Fe(III) (oxyhydr)oxides precipitated by the anaerobic nitrate-reducing Fe(II)-oxidizing *Acidovorax* sp. strain BoFeN1. *Geochim. Cosmochim. Acta* **2011**, *75*, 4699–4712.
- (15) Tufano, K. J.; Fendorf, S. Confounding impacts of iron reduction on arsenic retention. *Environ. Sci. Technol.* **2008**, *42* (13), 4777–4783.
- (16) Oloughlin, E. J.; Gorski, C. A.; Scherer, M. M.; Boyanov, M. I.; Kemner, K. M. Effects of oxyanions, natural organic matter, and bacterial cell numbers on the bioreduction of lepidocrocite ( $\gamma$ -FeOOH) and the formation of secondary mineralization products. *Environ. Sci. Technol.* **2010**, *44* (12), 4570–4576.
- (17) Piepenbrock, A.; Dippon, U.; Porsch, K.; Appel, E.; Kappler, A. Dependence of microbial magnetite formation on humic substance and ferrihydrite concentrations. *Geochim. Cosmochim. Acta* **2011**, *75* (22), 6844–6858.
- (18) Salas, E. C.; Berelson, W. M.; Hammond, D. E.; Kampf, A. R.; Nealon, K. H. The impact of bacterial strain on the products of dissimilatory iron reduction. *Geochim. Cosmochim. Acta* **2010**, *74* (2), 574–583.
- (19) Zachara, J. M.; Kukkadapu, R. K.; Fredrickson, J. K.; Gorby, Y. A.; Smith, S. C. Biomineralization of poorly crystalline Fe(III) oxides by dissimilatory metal reducing bacteria (DMRB). *Geomicrobiol. J.* **2002**, *19* (2), 179–207.
- (20) Chatellier, X.; West, M. M.; Rose, J.; Fortin, D.; Leppard, G. G.; Ferris, F. G. Characterization of iron-oxides formed by oxidation of ferrous ions in the presence of various bacterial species and inorganic ligands. *Geomicrobiol. J.* **2004**, *21* (2), 99–112.
- (21) Swanner, E. D.; Nell, R. M.; Templeton, A. S. *Ralstonia* species mediate Fe-oxidation in circumneutral, metal-rich subsurface fluids of Henderson mine, CO. *Chem. Geol.* **2011**, *284* (3–4), 339–350.
- (22) Chan, C. S.; De Stasio, G.; Welch, S. A.; Girasole, M.; Frazer, B. H.; Nesterova, M. V.; Fakra, S.; Banfield, J. F. Microbial polysaccharides template assembly of nanocrystal fibers. *Science* **2004**, *303* (5664), 1656–1658.
- (23) Larese-Casanova, P.; Haderlein, S. B.; Kappler, A. Biomineralization of lepidocrocite and goethite by nitrate-reducing Fe(II)-oxidizing bacteria: Effect of pH, bicarbonate, phosphate, and humic acids. *Geochim. Cosmochim. Acta* **2010**, *74* (13), 3721–3734.
- (24) Miot, J.; Benzerara, K.; Morin, G.; Kappler, A.; Bernard, S.; Obst, M.; Féraud, C.; Skouri-Panet, F.; Guigner, J.-M.; Posth, N.; Galvez, M.; Brown, G. E., Jr; Guyot, F. Iron biomineralization by anaerobic neutrophilic iron-oxidizing bacteria. *Geochim. Cosmochim. Acta* **2009**, *73* (3), 696–711.
- (25) Hegler, F.; Schmidt, C.; Schwarz, H.; Kappler, A. Does a low-pH microenvironment around phototrophic FeII-oxidizing bacteria prevent cell encrustation by FeIII minerals? *FEMS Microbiol. Ecol.* **2010**, *74* (3), 592–600.
- (26) Mikutta, C.; Frommer, J.; Voegelin, A.; Kaegi, R.; Kretzschmar, R. Effect of citrate on the local Fe coordination in ferrihydrite, arsenate binding, and ternary arsenate complex formation. *Geochim. Cosmochim. Acta* **2010**, *74* (19), 5574–5592.
- (27) Mikutta, C.; Mikutta, R.; Bonneville, S.; Wagner, F.; Voegelin, A.; Christl, I.; Kretzschmar, R. Synthetic coprecipitates of exopolysaccharides and ferrihydrite. Part I: Characterization. *Geochim. Cosmochim. Acta* **2008**, *72* (4), 1111–1127.
- (28) Jiang, J.; Kappler, A. Kinetics of microbial and chemical reduction of humic substances: Implications for electron shuttling. *Environ. Sci. Technol.* **2008**, *42* (10), 3563–3569.
- (29) Lovley, D. R.; Coates, J. D.; Blunt-Harris, E. L.; Phillips, E. J. P.; Woodward, J. C. Humic substances as electron acceptors for microbial respiration. *Nature* **1996**, *382* (6590), 445–448.
- (30) Wolf, M.; Kappler, A.; Jiang, J.; Meckenstock, R. U. Effects of humic substances and quinones at low concentrations on ferrihydrite reduction by *Geobacter metallireducens*. *Environ. Sci. Technol.* **2009**, *43* (15), 5679–5685.
- (31) Roden, E. E.; Kappler, A.; Bauer, I.; Jiang, J.; Paul, A.; Stoesser, R.; Konishi, H.; Xu, H. Extracellular electron transfer through microbial reduction of solid-phase humic substances. *Nat. Geosci.* **2010**, *3* (6), 417–421.
- (32) Konhauser, K. O. Diversity of bacterial iron mineralization. *Earth. Sci. Rev.* **1998**, *43* (3–4), 91–121.
- (33) Kleber, W.; Bausch, H.-J.; Bohm, J., *Einführung in die Kristallographie*, 19th ed.; Oldenbourg: München, 2010.
- (34) Myerson, A. S., *Handbook of Industrial Crystallization*, 2nd ed.; Butterworth-Heinemann: Woburn, 2002.
- (35) Hove, M.; Van Hille, R. P.; Lewis, A. E. The effect of different types of seeds on the oxidation and precipitation of iron. *Hydrometallurgy* **2009**, *97* (3–4), 180–184.
- (36) Charlet, L.; Bosbach, D.; Peretyashko, T. Natural attenuation of TCE, As, Hg linked to the heterogeneous oxidation of Fe(II): An AFM study. *Chem. Geol.* **2002**, *190* (1–4), 303–319.
- (37) Larese-Casanova, P.; Cwiertny, D. M.; Scherer, M. M. Nanogoethite formation from oxidation of Fe(II) sorbed on aluminum oxide: implications for contaminant reduction. *Environ. Sci. Technol.* **2010**, *44* (10), 3765–3771.

- (38) Peretyazhko, T.; Zachara, J. M.; Heald, S. M.; Kukkadapu, R. K.; Liu, C.; Plymale, A. E.; Resch, C. T. Reduction of Tc(VII) by Fe(II) Sorbed on Al (hydr)oxides. *Environ. Sci. Technol.* **2008**, *42* (15), 5499–5506.
- (39) Muehe, E. M.; Gerhardt, S.; Schink, B.; Kappler, A. Ecophysiology and the energetic benefit of mixotrophic Fe(II) oxidation by various strains of nitrate-reducing bacteria. *FEMS Microbiol. Ecol.* **2009**, *70* (3), 335–43.
- (40) Hegler, F.; Posth, N. R.; Jiang, J.; Kappler, A. Physiology of phototrophic iron(II)-oxidizing bacteria: implications for modern and ancient environments. *FEMS Microbiol. Ecol.* **2008**, *66* (2), 250–260.
- (41) Kappler, A.; Newman, D. K. Formation of Fe(III)-minerals by Fe(II)-oxidizing photoautotrophic bacteria. *Geochim. Cosmochim. Acta* **2004**, *68* (6), 1217–1226.
- (42) Jensen, D. L.; Boddum, J. K.; Tjell, J. C.; Christensen, T. H. The solubility of rhodochrosite (MnCO<sub>3</sub>) and siderite (FeCO<sub>3</sub>) in anaerobic aquatic environments. *Appl. Geochem.* **2002**, *17* (4), 503–511.
- (43) Stookey, L., Ferrozine - a new spectrometric reagent for iron. *Anal. Chem.* **1970**, *42*, (7).
- (44) Kukkadapu, R. K.; Zachara, J. M.; Fredrickson, J. K.; Kennedy, D. W.; Dohnalkova, A. C.; Mccready, D. E. Ferrous hydroxy carbonate is a stable transformation product of biogenic magnetite. *Am. Mineral.* **2005**, *90* (2–3), 510–515.
- (45) Weber, K. A.; Achenbach, L. A.; Coates, J. D. Microorganisms pumping iron: anaerobic microbial iron oxidation and reduction. *Nat. Rev. Microbiol.* **2006**, *4* (10), 752–764.
- (46) Chakraborty, A.; Roden, E. E.; Schieber, J.; Picardal, F. Enhanced growth of *Acidovorax* sp. strain 2AN during nitrate-dependent Fe(II) oxidation in batch and continuous-flow systems. *Appl. Environ. Microbiol.* **2011**, *77* (24), 8548–8556.
- (47) Jiao, Y.; Kappler, A.; Croal, L. R.; Newman, D. K. Isolation and characterization of a genetically tractable photoautotrophic Fe(II)-oxidizing bacterium, *Rhodospseudomonas palustris* strain TIE-1. *Appl. Environ. Microbiol.* **2005**, *71* (8), 4487–4496.
- (48) Weber, K. A.; Urrutia, M. M.; Churchill, P. F.; Kukkadapu, R. K.; Roden, E. E. Anaerobic redox cycling of iron by freshwater sediment microorganisms. *Environ. Microbiol.* **2006**, *8* (1), 100–113.
- (49) Pantke, C.; Obst, M.; Benzerara, K.; Morin, G.; Ona-Nguema, G.; Dippon, U.; Kappler, A. Green rust formation during Fe(II) oxidation by the nitrate-reducing *Acidovorax* sp. strain BoFeN1. *Environ. Sci. Technol.* **2012**, *46*, 1439–1446.
- (50) Miot, J.; Benzerara, K.; Morin, G.; Bernard, S.; Beyssac, O.; Larquet, E.; Kappler, A.; Guyot, F. Transformation of vivianite by anaerobic nitrate-reducing iron-oxidizing bacteria. *Geobiology* **2009**, *7* (3), 373–384.
- (51) Cornell, R. M.; Schwertmann, U., *The Iron Oxides: Structure, Properties, Reactions, Occurrence and Uses*, 2nd ed.; Wiley-VCH: Weinheim, 2003.
- (52) Schwertmann, U.; Fitzpatrick, R. W. Occurrence of lepidocrocite and its association with goethite in Natal soils. *Soil Sci. Soc. Am. J.* **1977**, *41* (5), 1013–1018.
- (53) Putnis, A., *Introduction to Mineral Sciences*; Cambridge University Press: Cambridge, 2003.
- (54) Bazylinski, D. A.; Frankel, R. B.; Konhauser, K. O. Modes of biomineralization of magnetite by microbes. *Geomicrobiol. J.* **2007**, *24* (6), 465–475.
- (55) Hansel, C. M.; Benner, S. G.; Fendorf, S. Competing Fe(II)-induced mineralization pathways of ferrihydrite. *Environ. Sci. Technol.* **2005**, *39* (18), 7147–7153.
- (56) Jiao, Y. Y. Q.; Kappler, A.; Croal, L. R.; Newman, D. K. Isolation and characterization of a genetically tractable photo autotrophic Fe(II)-oxidizing bacterium, *Rhodospseudomonas palustris* strain TIE-1. *Appl. Environ. Microbiol.* **2005**, *71* (8), 4487–4496.
- (57) Chaudhuri, S. K.; Lack, J. G.; Coates, J. D. Biogenic magnetite formation through anaerobic biooxidation of Fe(II). *Appl. Environ. Microbiol.* **2001**, *67* (6), 2844–2848.
- (58) Hansel, C. M.; Benner, S. G.; Neiss, J.; Dohnalkova, A.; Kukkadapu, R. K.; Fendorf, S. Secondary mineralization pathways induced by dissimilatory iron reduction of ferrihydrite under advective flow. *Geochim. Cosmochim. Acta* **2003**, *67* (16), 2977–2992.
- (59) Chan, C. S.; Fakra, S. C.; Edwards, D. C.; Emerson, D.; Banfield, J. F. Iron oxyhydroxide mineralization on microbial extracellular polysaccharides. *Geochim. Cosmochim. Acta* **2009**, *73* (13), 3807–3818.
- (60) Laresse-Casanova, P.; Scherer, M. M. Fe(II) sorption on hematite: New insights based on spectroscopic measurements. *Environ. Sci. Technol.* **2007**, *41* (2), 471–477.
- (61) Rosso, K. M.; Yanina, S. V.; Gorski, C. A.; Laresse-Casanova, P.; Scherer, M. M. Connecting observations of hematite ( $\alpha$ -Fe<sub>2</sub>O<sub>3</sub>) growth catalyzed by Fe(II). *Environ. Sci. Technol.* **2010**, *44* (1), 61–67.
- (62) Miot, J.; Maclellan, K.; Benzerara, K.; Boisset, N. Preservation of protein globules and peptidoglycan in the mineralized cell wall of nitrate-reducing, iron(II)-oxidizing bacteria: a cryo-electron microscopy study. *Geobiology* **2011**, *9*, 459–470.
- (63) Picardal, F. Abiotic and Microbial Interactions during Anaerobic Transformations of Fe and N. *Front. Microbiol.* **2012**, *3*.
- (64) Benali, O.; Abdelmoula, M.; Refait, P.; Génin, J.-M. R. Effect of orthophosphate on the oxidation products of Fe(II)-Fe(III) hydroxycarbonate: the transformation of green rust to ferrihydrite. *Geochim. Cosmochim. Acta* **2001**, *65* (11), 1715–1726.
- (65) Illes, E.; Tombacz, E. The effect of humic acid adsorption on pH-dependent surface charging and aggregation of magnetite nanoparticles. *J. Colloid Interface Sci.* **2006**, *295* (1), 115–123.
- (66) Kaiser, K.; Mikutta, R.; Guggenberger, G. Increased stability of organic matter sorbed to ferrihydrite and goethite on aging. *Soil. Sci. Soc. Am. J.* **2007**, *71* (3), 711–719.
- (67) Porsch, K.; Dippon, U.; Rijal, M. L.; Appel, E.; Kappler, A. In-situ magnetic susceptibility measurements as a tool to follow geomicrobiological transformation of Fe minerals. *Environ. Sci. Technol.* **2010**, *44* (10), 3846–3852.
- (68) Schwertmann, U.; Wagner, F.; Knicker, H. Ferrihydrite-humic associations: Magnetic hyperfine interactions. *Soil. Sci. Soc. Am. J.* **2005**, *69* (4), 1009–1015.